Med Biol Eng Comput (2015) 53:557–566
DOI 10.1007/s11517-015-1266-y

ORIGINAL ARTICLE

Correlation analysis of laser Doppler flowmetry signals: a potential non-invasive tool to assess microcirculatory changes in diabetes mellitus

Cerine Lal[1] · Sujatha Narayanan Unni[1]

Received: 5 February 2014 / Accepted: 27 February 2015 / Published online: 10 March 2015

Abstract Measurement and analysis of microcirculation is vital in assessing local and systemic tissue health. Changes in microvascular perfusion if detected can provide information on the development of various related diseases. Laser Doppler blood flowmetry (LDF) provides a non-invasive real-time measurement of cutaneous blood perfusion. LDF signals possess fractal nature that represents the correlation in the successive signal elements. Changes in the correlation of flow and its associated parameters could be used as a tool in differentiating the ailments at different stages or assessing the treatment effectiveness of a particular ailment. Spectral domain analysis of LDF signals reveals five characteristic frequency peaks corresponding to local and central regulatory mechanisms of the human body, namely metabolic, neurogenic, myogenic, respiration, and heart rate. This paper investigates the changes in the fractal nature and constituent frequency bands of laser Doppler signals in diabetic and healthy control subjects acquired from the glabrous skin of the foot so as to provide an assessment of microcirculatory dynamics. As a pilot study, it was attempted on a set of healthy control and diabetic volunteers, and the obtained results indicate that fractal nature of LDF signals is less in diabetic subjects compared to the healthy control. The wavelet analysis carried out on the set of signals reveals the dynamics of blood flow which may have led to the difference in correlation results.

Keywords Fractal · Wavelet transform · Hurst coefficient · Laser Doppler flow meter · Microcirculation · Diabetes

✉ Sujatha Narayanan Unni
nsujatha@iitm.ac.in

[1] Biophotonics Lab, Department of Applied Mechanics, Indian Institute of Technology Madras, Chennai 600036, India

1 Introduction

Diabetes mellitus (hereafter to be referred in this article as diabetes) is one of the most common chronic disease affecting nearly 200 million people worldwide and by 2025, it is estimated to increase affecting 333 million people globally as given by International Diabetic Federation (IDF) [24]. It is a group of metabolic diseases caused by altered blood sugar, either because the body does not produce enough insulin (Type 1) or because cells do not respond to the insulin that is produced (Type 2 which constitutes 90 % of diabetes worldwide). Blood flow dynamics has been actively considered as a potential tool for assessing diabetes for many years [5, 15, 28, 31, 35, 52]. Of these, microcirculation also has been actively investigated for the purpose specifically [4, 14, 15, 31, 32, 47, 53]. Impaired flow to lower limbs reflected in the foot sole is a common microcirculatory complication faced by diabetic patients which leads to gangrene and even amputation if left untreated. Succeeding health problems include ulceration in the lower extremities, neuropathy, an impaired blood supply, and hypertension. Previous studies have shown the role of microvascular change in the pathogenesis of diabetes with respect to metabolism [10, 23], effect of nitric oxide (NO) [44], peripheral microvascularization changes [46], dermal neurovascular dysfunction [49], microvascular dysfunction [6, 26, 39, 40], and venous distension [50].

LDF, a technique based on the frequency shift of incoming and outgoing laser to/from the tissue to assess the flow velocity based on red blood cell scattering, provides a real-time non-invasive measurement of microvascular perfusion [8, 9]. LDF measures local cutaneous blood perfusion, which is affected by cardiac pumping, respiration, influence of the autonomic nervous system, and local metabolism. Different signal processing strategies have been adopted

for analysing LDF signals previously for essentially facilitating flow velocity [33]. Dynamic characteristics of laser Doppler flux have been investigated previously [37]. Considering the complexity of the interactions that determine the microvascular perfusion, temporal fluctuations in the LDF signals can be characterized by fractal analysis, a technique that is capable of characterizing irregular time series generated from nonlinear systems [13, 17, 18]. Self-similar nature of LDF signals at different scales of observation is indicated by a frequency spectrum having a form of an inverse power–law relationship. The extent of this self-similarity is measured by Hurst coefficient (H) which is a measure of the extent of correlation between successive elements of the time series. Various methods are available for estimating the fractal characteristics of a time series. Important methods include Hurst rescaled range analysis, variogram method, dispersional analysis, scaled windowed variance, detrended fluctuation analysis, and box counting method [12, 21, 22, 27, 34]. Application studies involving LDF data from rat brain cortex and volar surface of forearm have been found to possess fractal characteristics previously [12, 13, 20, 33].

Decomposing LDF signals in the spectral domain reveals various physiological rhythms associated with blood flow control mechanisms [11, 30]. Unlike Fourier transform, short-time Fourier transform (STFT) and wavelet transform (WT) simultaneously retain time and frequency information. STFT gives the time–frequency content of a signal with a constant frequency and time resolution due to the fixed window length, whereas continuous WT retrieves the time–frequency content information with an improved resolution due to its multiresolution property [16]. Continuous wavelet transform (CWT) is used to analyse the scale-dependent structure of a signal as it varies in time. In this article, the CWT is considered as a qualitative tool to analyse LDF signals. As the frequencies contained in the LDF are low frequencies, to obtain good low-frequency resolution wavelet analysis is preferred over Fourier and STFT as it offers good frequency and time resolution. Previously, wavelet analysis of LDF signals from human forearm has revealed five characteristic frequency bands corresponding to various physiological mechanisms, namely cardiogenic activity (0.6–1.6 Hz) representing the heart beat dynamics; respiratory (0.15–0.4 Hz) the rhythmicity of breath; myogenic activity (0.06–0.15 Hz) the rhythmic activity of vessels; neurogenic activity (0.02–0.06 Hz); and endothelial activity (0.0095–0.02 Hz) corresponding to metabolic activity [7, 30, 43, 45]. The relative contribution of power spectral density of these bands is an indicative of underlying vascular functioning and reactivity. Changes in vascular function are associated with diseases like hypertension, peripheral vascular disease, and diabetes.

In this pilot study, LDF signals obtained from the glabrous skin of the plantar area of the foot of the Type 2 diabetic subjects are first subjected to fractal analysis to estimate the correlation in a gross level, and the amount of signal correlation is further investigated by WT analysis to assess the changes in the associated capillary blood flow dynamics associated with the disease.

2 Materials and methods

2.1 Experimental set-up

Blood perfusion signals were recorded using ML-191 model laser Doppler blood flow meter (AD Instruments Inc., Australia, operating at 830 $\pm$ 10 nm and 0.5 mW). An optical fibre probe connected with the ML-191 (Oxy-Flo, Oxford Optronix Ltd) was used to illuminate and collect the scattered light from the skin tissue. The probe was attached to the surface of interest by means of a two-sided adhesive tape. The instrument calculates the blood perfusion or red blood cell flux in arbitrary units which is represented as the product of RBC concentration and scatterer velocity under the probed volume. The flow meter was connected to the PowerLab® data acquisition system which used LabChart® software for data acquisition.

The study was conducted on six Type 2 diabetic subjects without neuropathy and an equal number of healthy control subjects. Subjects with smoking habits and alcoholics were excluded from the study. Also, subjects with neuropathy/necrotic ulcers were not considered for this pilot study. The average age of control group was 41 with a standard deviation of 15 and that of the diabetic group was 50 with a standard deviation of 6.9. All the subjects were asked to clean their foot, and the measurement was taken from the metatarsal region of the foot uniformly. The selection of metatarsal region as the region of interest was made based on previous research on diabetic foot to extract oxygenation flow details by our group [1]. Also, this region is one among the regions in the foot sole, prone to develop ulcer with the more predominant changes in flow dynamics due to exerted walking pressure.

The region of interest was confirmed free from callus formation before taking the measurement. The measurements were taken with the subjects in the supine position with their foot allowed in a resting position throughout the measurement. The subjects who participated in the study were fully informed of experimental procedures, protocol, and purpose associated with the study. The participation in this study was purely voluntary with the subjects' written consent. The study was approved by the Institute Ethics Committee, IIT Madras. The experimental set-up for LDF

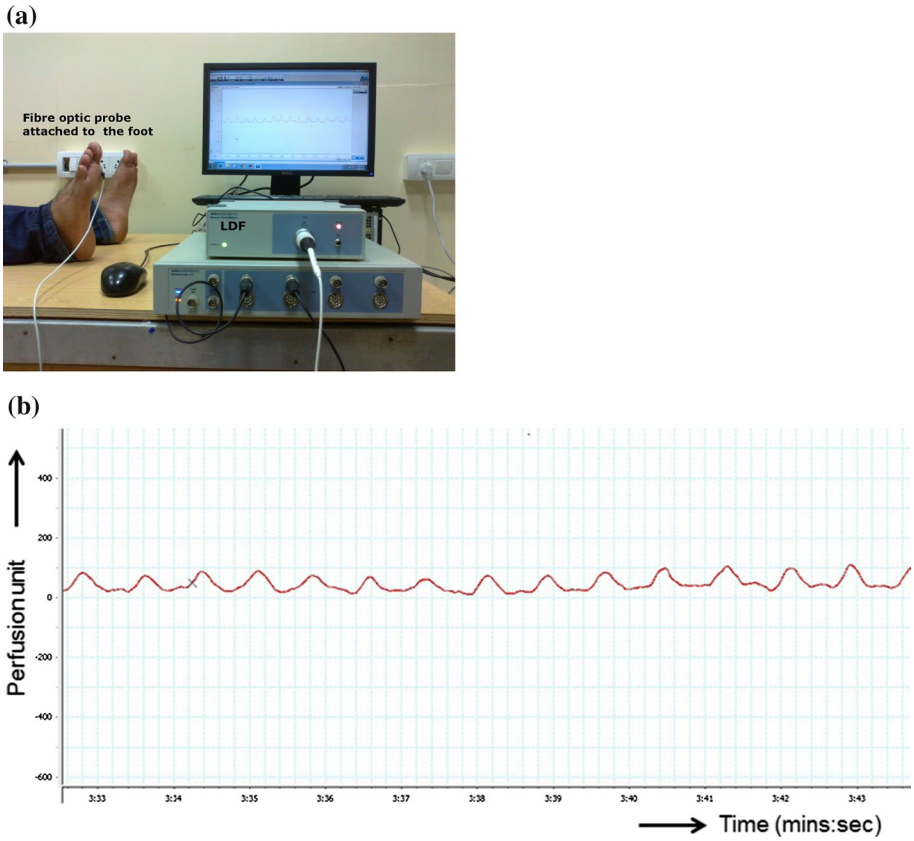

Fig. 1 **a** Laser Doppler flow meter (LDF) experimental set-up: The system consists of the laser unit, optical fibre probe for illumination and collection, and a data acquisition/processing unit. The obtained perfusion signal is also shown. **b** Recorded perfusion signal shown separately

measurements is shown in Fig. 1a, and a sample recorded LDF signal is shown in Fig. 1b.

2.2 Fractal analysis

For all the subjects, LDF signals were recorded for 20 min duration at a sampling rate of 1 kHz using the experimental set-up from the plantar area of the foot. Signals of 5 min duration were considered for the study involving fractal analysis. The fractal nature of the LDF signals was checked by power spectrum analysis, and the log power spectral density versus log frequency curve is found to obey a power–law relationship given as below.

$$P(f) = \frac{1}{f^{\beta}} \tag{1}$$

where f is the frequency and β is the slope of the log–log plot as shown in Fig. 2. The obtained values of β for all the recorded signals showed that the nature of the signals is fractional Brownian motion, where $\beta > 1$ [12].

Variability of fractional Brownian motion LDF signals at different scales was analysed using line detrended scaled windowed variance technique to estimate the Hurst coefficient (H). In order to get an accurate estimate of H with 0.95 probability of distinguishing between two time series with H differing by 0.1, 2^{18} points of the signal

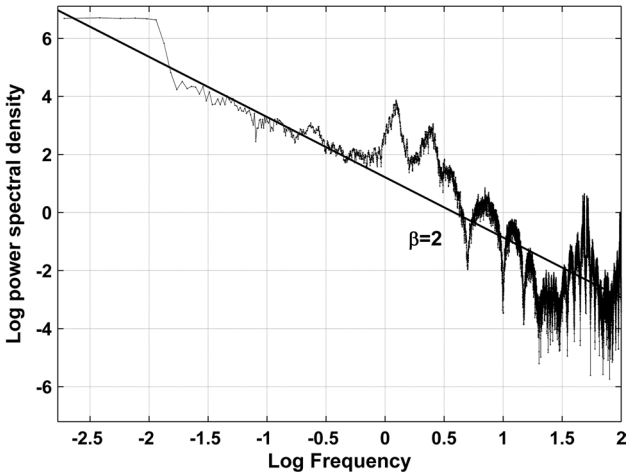

Fig. 2 Log power spectral density versus log frequency plot of recorded perfusion signals obeying the power–law

were considered while doing scaled variance analysis [12].

In line detrended scaled windowed variance method, the LDF data are divided into non-overlapping windows of size $n(n = 2^4, 2^5 \ldots 2^{10})$. Too small and too large window sizes were not used for optimum results [12]. For each of these window sizes, a least square fit is calculated for the points

in each window, and this linear fit is then subtracted from the points within these windows. Then, the average local standard deviation (SD) for each of these windows is calculated, and the mean of the SD for that particular window size n is found. This is repeated for all window sizes. A plot of log SD against log window size (n) is made. The slope of the least squares fit to the plot gives the Hurst coefficient (H).

2.2.1 Significance of H

H can be any real number in the range $0 < H < 1$. H indicates whether the signal has a persistent or anti-persistent behaviour. $H > 0.5$ indicates a persistent signal implying that the increments of the series are correlated. In a correlated series, it is more likely that a positive increment follows a positive increment or that a negative increment follows a negative increment. $H < 0.5$ indicates increments of the signal that is anti-correlated. Anti-correlated series have successive increments that follow alternate ups and downs [2, 13, 17, 18, 41].

2.3 Wavelet analysis

For the wavelet analysis, the complete signal for the duration of 20 min was used. CWT is a scale-independent method used to analyse the time–frequency characteristics of wide band, non-stationary signals. The CWT uses a mother wavelet and by scaling and translating the mother wavelet along the length of the signal, the WT performs the time scale decomposition thus providing time localization and multiresolution capability. The CWT of a signal $f(t)$ is defined as

$$F(\tau, s) = \frac{1}{\sqrt{|s|}} \int_{-\infty}^{\infty} f(t)\, \varphi^* \left(\frac{t-\tau}{s} \right) \mathrm{d}t \tag{2}$$

where s is the scaling and τ is the translational parameter of the mother wavelet φ [16, 19]. In this paper, we have used complex Morlet wavelet which is based on Gaussian window modulated by sine wave for the analysis of LDF signals as it has the best representation in both time and frequency. The Gaussian function guarantees a minimum time-bandwidth product, providing simultaneous localization in both time and frequency domains. It has been used as a mother wavelet for signals that require high-frequency resolution at low frequencies like LDF [42].

Complex Morlet in time domain is defined as

$$\varphi(t) = \frac{1}{\sqrt{\pi f_\mathrm{b}}} e^{i 2\pi f_\mathrm{c} t} e^{\frac{-t^2}{f_\mathrm{b}}} \tag{3}$$

where f_b is the bandwidth parameter, f_c is the wavelet centre frequency, and $\varphi(t)$ represents the wavelet coefficients at time t [38]. For the analysis of LDF signals, complex Morlet with f_c 1 Hz and f_b of 2 was used.

The processing of LDF signals was carried out using MATLAB Signal Processing Toolbox. Prior to the wavelet analysis, the signals were mean subtracted and resampled at 10 Hz after applying a low-pass filter to prevent anti-aliasing. After down sampling, the signal was high-pass-filtered to remove low-frequency signals below 0.005 Hz. Also, to eliminate end effects while computing WT, the pre-processed LDF signal was negatively reflected about its ends. After pre-processing the LDF signals, CWT was computed, and the average energy density in each frequency band was analysed from the obtained wavelet scalogram. Average energy density in each band ($\in (f_1, f_2)$) is given by Eq. (4),

$$(\in (f_1, f_2)) = \frac{1}{t} \int_0^t \int_{s_1}^{s_2} \frac{1}{s^2} |g(s,t)|^2 \mathrm{d}s\mathrm{d}t \tag{4}$$

where f_1, f_2 are the lower and upper limit of the frequency band of interest, s_1, s_2 are the scales corresponding to f_1 and f_2, and $g(s,t)$ is the CWT of the LDF signal at scale s and time t. For a signal sampled with sampling period Δ, the scale s of the Morlet wavelet is related to the frequency f(Hz) as given in Eq. (5),

$$f = \frac{f_\mathrm{c}}{\Delta s} \tag{5}$$

Hence, in order to analyse the LDF signals sampled at 10 Hz and for a frequency range of 0.005–2.5 Hz using Morlet wavelet with f_c 1 Hz, scale s was varied from 4 to 2000.

3 Results

The LDF experiments were carried out as detailed in Sect. 2. The acquired signals from healthy control and diabetic subjects were subjected to fractal analysis as well as wavelet analysis. The details of the results obtained for each analysis are as listed below.

3.1 Fractal analysis

Hurst coefficient for the LDF signals was computed as per Sect. 2.2. Sample plots illustrating the computation of H in the case of healthy control as well as diabetic subjects are shown in Fig, 3a, b. In the diabetic group, $H = 0.700 \pm 0.0379$ (mean $\pm$ SE), whereas in the healthy group, $H = 0.810 \pm 0.0044$ (mean $\pm$ SE) as shown in Fig. 4. The Hurst coefficient is observed to be less in the case of diabetic subjects when compared to healthy control subjects. We observed the following correlation coefficient in the LDF time series of the diabetes subjects and in healthy subjects.

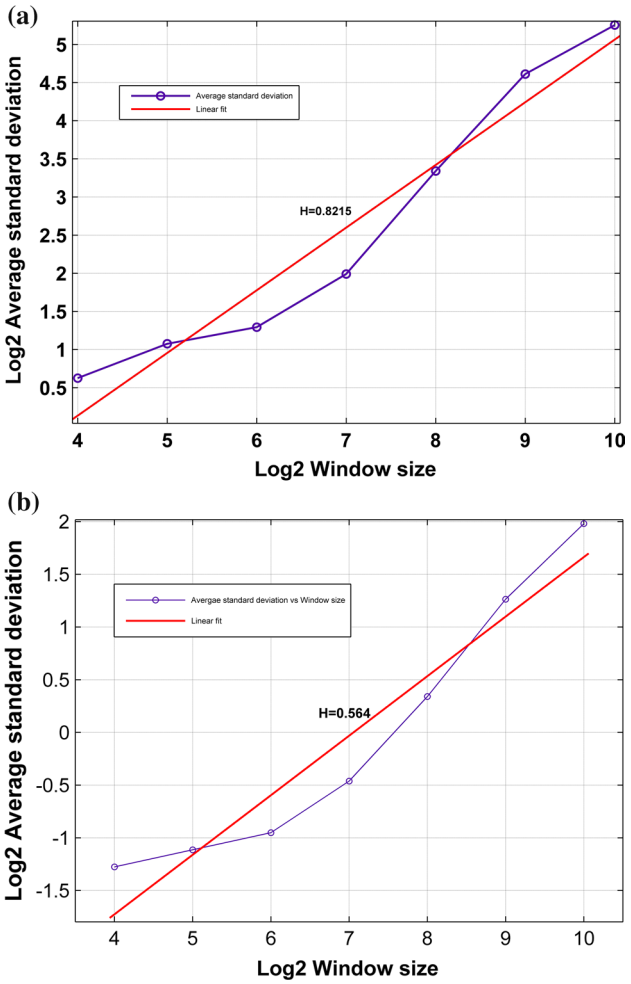

Fig. 3 Plot of scaled windowed variance analysis, **a** healthy control subject, **b** diabetic subject

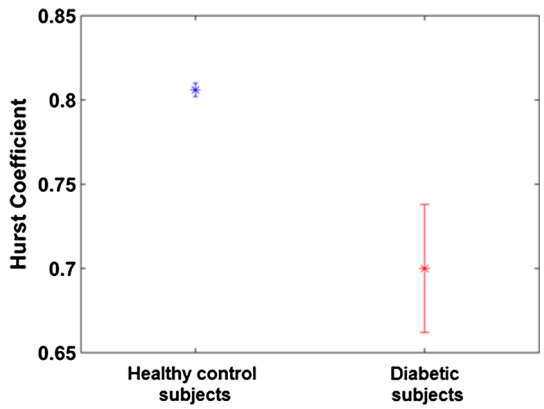

Fig. 4 Graph showing Hurst coefficient (mean ± SE) in healthy control and diabetic subjects

3.2 Wavelet analysis

Figure 5a, b shows the average WT coefficients of LDF signals with their five characteristic peaks in the corresponding frequency bands in healthy control and diabetic subjects, respectively.

To quantitatively measure the changes in dynamics in different frequency bands, the relative energy contribution of each band to the total average energy density in the band 0.0095–2.5 Hz was used and is observed to be an indicator of changes in underlying control mechanisms of microcirculation.

Wavelet analysis has revealed significant results between the different frequency bands associated with underlying blood flow control mechanism. The average relative power of different bands in the healthy controls and diabetic subjects was analysed. It was found that the changes occurring in the metabolic band, neurogenic band, and cardiac band are significant and can be used to assess the dynamics of microcirculation in diabetic subjects. In the healthy control subjects, the average relative power in the metabolic and neurogenic bands is found to have reduced value as compared to their diabetic counterparts, and an opposite trend was observed in the cardiac band. While these changes are found to be significant, there was no significant difference observed in the myogenic and respiratory bands between the two groups. Also, we observed that the ratio of relative energy in cardiac band to metabolic band and the ratio of cardiac band to neurogenic band differed possibly significantly between diabetic and healthy control subjects. The percentage relative energy for each band/band ratios for healthy control subjects as well as diabetic subjects is shown in Fig. 6.

4 Discussions

The diabetic group selected for the study varied in their degree of impairment, and hence, an increased standard error was observed in the group. In the fractal analysis, the diabetic group shows significant deviation ($p < 0.05$ by two-tailed t test) in the Hurst exponent from the healthy control group. Some of the diabetic subjects showed $H = 0.56$ which is close to Brownian motion indicating random walk like fluctuations, whereas for healthy control subjects, we have observed $H > 0.8$ consistently. H indicates the strength of correlation between successive elements in the LDF time series. The mean value of H for the diabetic group and healthy control group was >0.5 indicating positive correlation between successive elements. However, the calculated

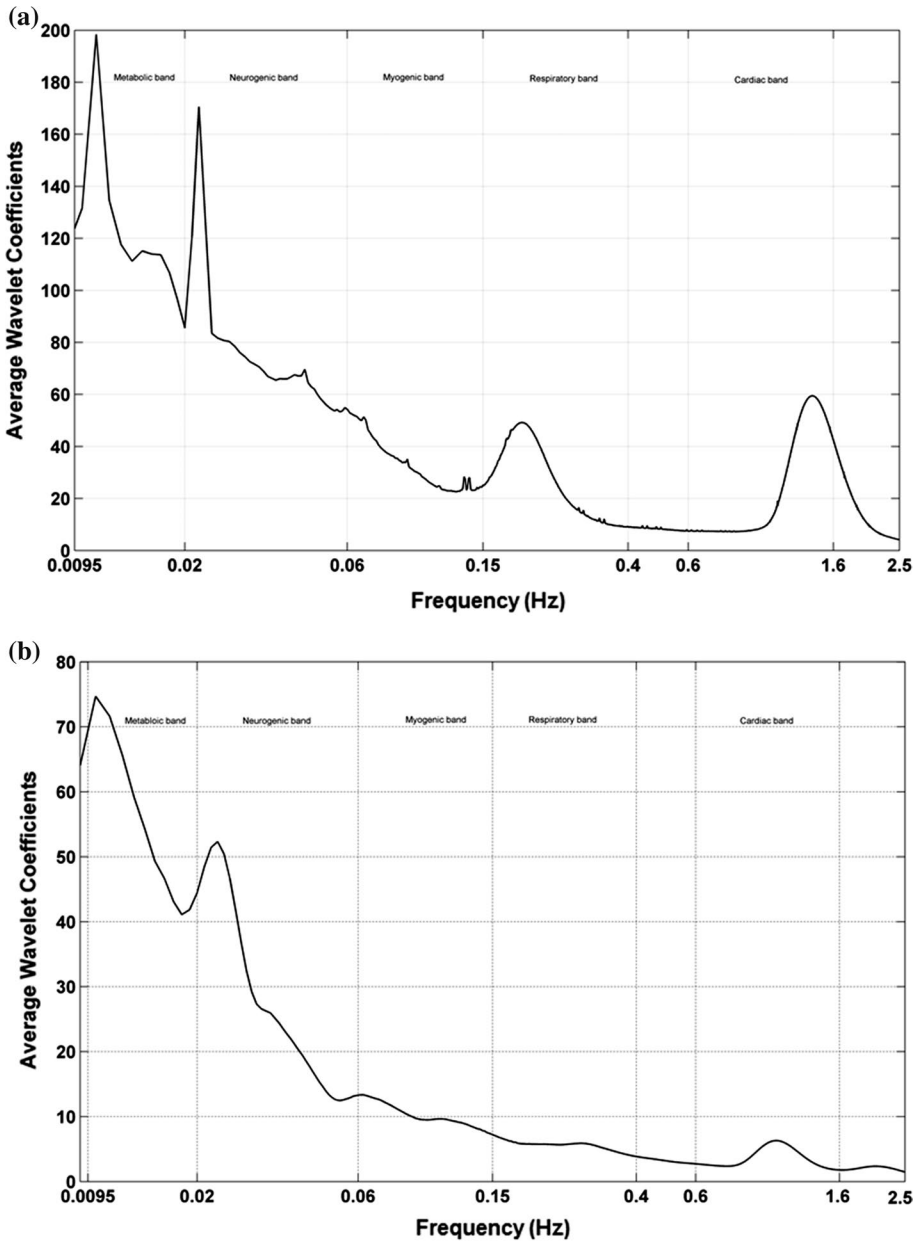

Fig. 5 Plot of time averaged wavelet transform coefficient, **a** healthy control subject, **b** diabetic subject

H was more for the healthy control group than the diabetic indicating that the increments of the LDF time series are more positively correlated in healthy control subjects than in the diabetic subjects. The results indicate that flow pattern in healthy control subjects is more correlated than that of diabetic subjects. This decrease in H in diabetic subjects could be due to the microcirculatory changes associated with diabetes. Also, some of the diabetic subjects showed $H = 0.56$ which indicates uncorrelated or random fluctuations of the LDF time series suggesting loss of coordination of the mechanisms governing blood flow, namely metabolic, neurogenic, myogenic, respiratory, and cardiac components. Similar observations were made in case of wavelet analysis as mentioned Sect. 3.2, leading to an inference that the changes in the Hurst coefficient in LDF signals between the diabetic and healthy control group are attributed to the changes in the underlying microcirculation as indicated by wavelet analysis. The possible causes for the differences in various frequency bands of the LDF signal for the healthy control and diabetic subjects are further analysed as below.

4.1 Neurogenic band

In our experiments, we have observed that for the healthy control subjects, the average relative energy in this band [0.02–0.06 Hz] was observed to be 0.1803 ± 0.0293, whereas for the diabetic group, the value was found to be 0.2653 ± 0.0356. The difference was observed to

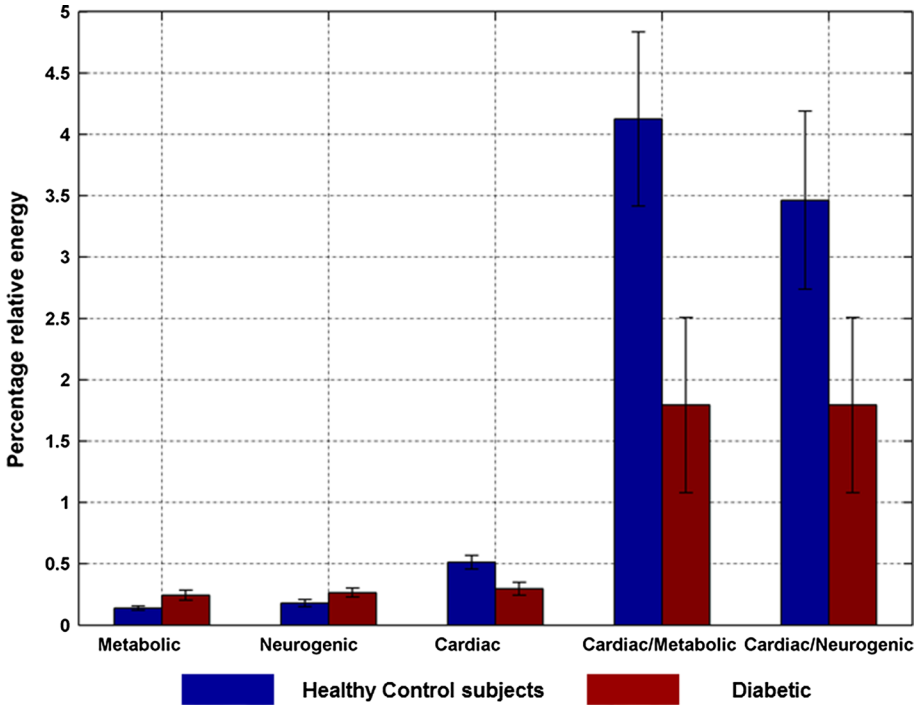

Fig. 6 Bar graph showing relative energy distribution in various bands/band ratios in diabetes and healthy control subjects

be statistically significant with a p value of 0.0258. In humans, Stefanovska et al. [7, 29, 43] observed that introduction of acetylcholine (vasodilator) into the subjects caused decrease in the relative energy of neurogenic band. Hence, the observed increase in the relative energy in the neurogenic band in diabetic group compared to healthy control subjects can be due to the vasoconstriction of the blood vessels. It is shown that diabetes increases the production of vasoconstrictors mainly endothelin-1 which acts on vascular smooth muscle inducing vasoconstriction along with decrease in the production of endothelium-derived NO thus impairing endothelium dependant vasodilation [26, 48]. Also, studies show that patients with diabetes tend to have decreased cutaneous vasodilation and impaired sympathetic neural control [44, 49]. The above factors correspond to the increased relative contribution of neurogenic oscillations in the cutaneous perfusion in diabetic subjects.

4.2 Cardiac band

We observed that in diabetic subjects, the relative energy contribution in the cardiac region [0.6–2 Hz] to the total blood flow was less when compared to healthy control subjects. For the healthy control subjects, the average relative energy was observed to be 0.5126 ± 0.0559, whereas for the diabetic group, the value was found to be 0.2953 ± 0.0525. A possible cause for this finding is that increased vessel resistance due to vasoconstriction leads to decrease in the contribution of heart to total microcirculatory flow. It is also shown in the literature that injection of vasodilator causes an increase in the contribution of cardiac component to the total blood flow due to vasodilatation [43, 45]. Hence, the decrease in relative energy in this band is attributed to increased vessel resistance due to vasoconstriction. Also, this observed change was statistically significant ($p = 0.0175$).

4.3 Metabolic band

In the frequency band from 0.0095 to 0.16 Hz, peak is observed at 0.01 Hz that corresponds to endothelial cell metabolic activity [7, 30]. Endothelial cells that line the inner surface of the blood vessels regulate vasomotor tone by production of vasodilator mediators. Therefore, variations in this band can indicate either the rate of release of various vasoactive substances or the response of the endothelial cells to these substances. Endothelial dysfunction associated with diabetes is characterized by impaired regulation of vasodilation due to decreased production of NO [3, 25, 36, 51]. NO plays a major role in vasodilation and blood pressure regulation of blood vessels. For the healthy control subjects, the average relative energy was observed to be 0.1382 ± 0.0181, whereas for the diabetic group, the value was found to be 0.2444 ± 0.049. The observed increase in the relative energy contribution of this band in diabetic subjects compared to healthy control subjects was found to be statistically significant ($p = 0.0635$) and expected to be due to the effects of endothelial dysfunction.

4.4 Band ratio

The ratio of relative energies in cardiac band to metabolic band (healthy controls—4.1267 ± 0.7096: diabetic—1.7935 ± 0.7149; $p = 0.0988$) and cardiac band to neurogenic band (healthy controls—3.4625 ± 0.7257: diabetic—1.6409 ± 0.7068; $p = 0.0425$) was additionally calculated and found to be a better prominent marker for differentiating diabetic subjects from the control group. Although the ratio of cardiac to metabolic band was not an evidently significant marker from the p values, we feel that there is a potential for exploring further in this direction by conducting experiments in a large subject group. This could potentially serve as an effective indicator of the disease stages after proper experimental trials on a large population.

The summary of results obtained in this study shows that the fractal nature of the LDF signals as described by Hurst coefficient differs considerably in diabetic and healthy control subjects. This change in fractal nature is due to the pathophysiological changes associated during the development of diabetes as shown by wavelet analysis of the LDF signals. The differences obtained in the cardiac, neurogenic, and metabolic band indicate that diabetes leads to the vasoconstriction of the capillaries causing reduced blood flow to the tissues.

5 Conclusion

In this pilot study, microcirculatory changes associated with diabetes mellitus is studied employing temporal fractal analysis of laser Doppler signals. The results indicate that Hurst coefficient which describes the strength of correlation between successive elements of the LDF time series showed statistically significant reduction in diabetic subjects compared to the healthy control group. For further analysis, signals were acquired at greater duration and subjected to wavelet analysis to understand the changes in the underlying vascular control mechanisms associated with diabetes. The introduction of ratios between cardiac, myogenic, and neurogenic bands clearly differentiates the healthy control group from the patients' group. Results from wavelet analysis were found to be in favour of the results from fractal analysis that yielded more detailed information. Hence, it is concluded that fractality of the Doppler signals could offer a promising tool to be used as another modality for preliminary screening of ailments involving microcirculatory changes hence can be used as a non-invasive tool for disease assessment in comparatively reduced test time.

Acknowledgements The authors acknowledge the financial help from the Indian Institute of Technology Madras for carrying out the study. All the volunteers from the Institute hospital who participated in this study are also greatly acknowledged.

References

1. Anand S, Sujatha N, Narayanamurthy VB, Seshadri V, Poddar R (2014) Diffuse reflectance spectroscopy for monitoring diabetic foot ulcer—a pilot study. Opt Lasers Eng. doi:10.1016/j.optlaseng.2013.07.020
2. Arakelyan SM, Kucherik AO, Prokoshev VG, Troitskii DP, Shishkina MV (2010) Nonlinear signal processing of laser Doppler flowmetry records. Biomed Technol Radio Electron 7:29–32
3. Bakker W, Eringa EC, Sipkema P, van Hinsbergh VW (2009) Endothelial dysfunction and diabetes: roles of hyperglycemia, impaired insulin signaling and obesity. Cell Tissue Res 335(1):165–189. doi:10.1007/s00441-008-0685-6
4. Barnes MD, Peppiatt TN, Mani R (1991) Glimpses into measurements of the microcirculation in skin. In: 30th Annual meeting of the biological engineering society, 18 Sept 1990–20 Sept 1990, Durham, NC, USA, J Biomed Eng, pp 185–188
5. Bernjak A, Stefanovska A, Urbancic-Rovan V, Azman-Juvan K (2005) Quantitative assessment of oscillatory components in blood circulation: classification of the effect of aging, diabetes, and acute myocardial infarction. In: Advanced biomedical and clinical diagnostic systems III, 23 Jan 2005, USA. Proceedings of the SPIE International Society Optics Engineering (USA). SPIE Int Soc Opt Eng, pp 163–173. doi:10.1117/12.589572
6. Bondar IA, Klimontov VV, Korolyova EA (2002) Autonomic neuropathy in diabetes: early detection and the role in development of microvascular complications. In: Proceedings 6th Russian-Korean international symposium on science and technology, 24–30 June 2002, Piscataway, NJ, USA, Proceedings 6th Russian-Korean international symposium on science and technology. KORUS-2002 (Cat. No. 02EX565). IEEE, pp 464–467. doi:10.1109/KORUS.2002.1028065
7. Bračič M, Stefanovska A (1998) Wavelet-based analysis of human blood-flow dynamics. Bull Math Biol 60(5):919–935. doi:10.1006/bulm.1998.0047
8. Braverman IM (2000) The cutaneous microcirculation. J Investig Dermatol Symp Proc 5(1):3–9. doi:10.1046/j.1087-0024.2000.00010.x
9. Briers JD (2001) Laser Doppler, speckle and related techniques for blood perfusion mapping and imaging. Physiol Meas 22(4):R35–R66
10. Cameron NE, Eaton SE, Cotter MA, Tesfaye S (2001) Vascular factors and metabolic interactions in the pathogenesis of diabetic neuropathy. Diabetologia 44(11):1973–1988. doi:10.1007/s001250100001
11. Campos R, Figueiras E, Ferreira LFR, Humeau-Heurtier A (2012) Spectral analysis of laser Doppler flowmetry signals. In: Bioengineering (ENBENG), 2012 IEEE 2nd Portuguese meeting in, 23–25 Feb 2012, pp 1–6. doi:10.1109/ENBENG.2012.6331342
12. Cannon MJ, Percival DB, Caccia DC, Raymond GM, Bassingthwaighte JB (1997) Evaluating scaled windowed variance methods for estimating the Hurst coefficient of time series. Phys A 241(3–4):606–626. doi:10.1016/s0378-4371(97)00252-5
13. Carolan-Rees G, Tweddel AC, Naka KK, Griffith TM (2002) Fractal dimensions of laser Doppler flowmetry time series. Med Eng Phys 24(1):71–76
14. Chih-Hui H, Eng-Kean Y, Kang-Ping L (2003) Portable laser Doppler flowmetry in studying the effect of diabetes mellitus on cutaneous microcirculation. J Med Biol Eng 23(1):13–18
15. Cobb JE, Claremont DJ (2002) In-shoe measurement of plantar blood flow in diabetic subjects: results of a preliminary clinical evaluation. Physiol Meas 23(2):287–299. doi:10.1088/0967-3334/23/2/305

16. De Moortel I, Munday SA, Hood AW (2004) Wavelet analysis: the effect of varying basic wavelet parameters. Sol Phys 222(2):203–228. doi:10.1023/B:SOLA.0000043578.01201.2d
17. Eke A, Herman P, Bassingthwaighte JB, Raymond GM, Percival DB, Cannon M, Balla I, Ikrenyi C (2000) Physiological time series: distinguishing fractal noises from motions. Pflug Arch 439(4):403–415
18. Eke A, Herman P, Kocsis L, Kozak LR (2002) Fractal characterization of complexity in temporal physiological signals. Physiol Meas 23(1):R1–R38
19. Galli AW, Heydt GT, Ribeiro PF (1996) Exploring the power of wavelet analysis. Comput Appl Power IEEE 9(4):37–41. doi:10.1109/67.539845
20. Glenny RW, Robertson HT, Yamashiro S, Bassingthwaighte JB (1991) Applications of fractal analysis to physiology. J Appl Physiol (Bethesda, MD: 1985) 70(6):2351–2367
21. Goldberger AL, Amaral LA, Hausdorff JM, Ivanov P, Peng CK, Stanley HE (2002) Fractal dynamics in physiology: alterations with disease and aging. Proc Natl Acad Sci USA 99(Suppl 1):2466–2472. doi:10.1073/pnas.012579499
22. Goldberger AL, West BJ (1987) Fractals in physiology and medicine. Yale J Biol Med 60(5):421–435
23. Greenman RL, Panasyuk S, Wang X, Lyons TE, Dinh T, Longoria L, Giurini JM, Freeman J, Khaodhiar L, Veves A (2005) Early changes in the skin microcirculation and muscle metabolism of the diabetic foot. Lancet 366(9498):1711–1717. doi:10.1016/s0140-6736(05)67696-9
24. IDF Diabetic Atlas (2013) 6th edition International Diabetes Federation
25. James PE, Lang D, Tufnell-Barret T, Milsom AB, Frenneaux MP (2004) Vasorelaxation by red blood cells and impairment in diabetes: reduced nitric oxide and oxygen delivery by glycated hemoglobin. Circ Res 94(7):976–983. doi:10.1161/01.res.0000122044.21787.01
26. Kalani M (2008) The importance of endothelin-1 for microvascular dysfunction in diabetes. Vasc Health Risk Manag 4(5):1061–1068
27. Klinkenberg B (1994) A review of methods used to determine the fractal dimension of linear features. Math Geol 26(1):23–46. doi:10.1007/BF02065874
28. Kun H, Peng CK, Huang NE, Zhaohua W, Lipsitz LA, Cavallerano J, Novak V (2008) Altered phase interactions between spontaneous blood pressure and flow fluctuations in type 2 diabetes mellitus: nonlinear assessment of cerebral autoregulation. Phys A 387(10):2279–2292. doi:10.1016/j.physa.2007.11.052
29. Kvandal P, Stefanovska A, Veber M, Kvernmo HD, Kirkeboen KA (2003) Regulation of human cutaneous circulation evaluated by laser Doppler flowmetry, iontophoresis, and spectral analysis: importance of nitric oxide and prostaglandines. Microvasc Res 65(3):160–171
30. Kvernmo HD, Stefanovska A, Bracic M, Kirkebøen KA, Kvernebo K (1998) Spectral analysis of the laser Doppler perfusion signal in human skin before and after exercise. Microvasc Res 56(3):173–182. doi:10.1006/mvre.1998.2108
31. Liu D, Wood NB, Xu XY, Witt N, Hughes AD, Thom SA (2008) Image-based blood flow simulation in the retinal circulation. In: 4th European conference of the international federation for medical and biological engineering, ECIFMBE 2008, 23 Nov 2008–27 Nov 2008, Antwerp, Belgium, 2008. IFMBE Proceedings. Springer, Berlin, pp 1963–1966. doi:10.1007/978-3-540-89208-3_468
32. Meglinski IV Diffusing wave spectroscopy and its application for monitoring of skin blood microcirculation. In: Saratov Fall Meeting 2002 Optical Technologies in Biophysics and Medicine IV, 1 Oct 2002–4 Oct 2002, Saratov, Russia, 2002. Proceedings of SPIE—the International Society for Optical Engineering. SPIE, pp 163–169. doi:10.1117/12.518758
33. Obeid AN (1993) In vitro comparison of different signal processing algorithms used in laser Doppler flowmetry. Med Biol Eng Comput 31(1):43–52
34. Peng CK, Havlin S, Stanley HE, Goldberger AL (1995) Quantification of scaling exponents and crossover phenomena in nonstationary heartbeat time series. Chaos (Woodbury, NY) 5(1):82–87. doi:10.1063/1.166141
35. Petrofsky J (2011) A method of measuring the interaction between skin temperature and humidity on skin vascular endothelial function in people with diabetes. J Med Eng Technol 35(6–7):330–337. doi:10.3109/03091902.2011.592237
36. Pieper GM (1998) Review of alterations in endothelial nitric oxide production in diabetes: protective role of arginine on endothelial dysfunction. Hypertension 31(5):1047–1060
37. Popivanov D, Mineva A, Bendayan P, Leger P, Boccalon H, Moller KO (1999) Dynamic characteristics of laser-Doppler flux in normal individuals and patients with Raynaud's phenomenon before and after treatment with nifedipine under different thermal conditions. Technol Health Care 7(2/3):193–203
38. Rioul O, Vetterli M (1991) Wavelets and signal processing. Sig Process Mag IEEE 8(4):14–38. doi:10.1109/79.91217
39. Sancho RAS, Pastore GM (2012) Evaluation of the effects of anthocyanins in type 2 diabetes. Food Res Int 46(1):378–386. doi:10.1016/j.foodres.2011.11.021
40. Sanka SC, Bennett DC, Rojas JD, Tasby GB, Meininger CJ, Wu G, Wesson DE, Pfarr C, Martinez-Zaguilan R (2000) Ca^{2+} homeostasis in microvascular endothelial cells from an insulin dependent diabetic model: role of endosomes/lysosomes. In: Proceedings of SPIE—the International Society for Optical Engineering, vol 3924, pp 56–66
41. Shiogai Y, Stefanovska A, McClintock PV (2010) Nonlinear dynamics of cardiovascular ageing. Phys Rep 488(2–3):51–110. doi:10.1016/j.physrep.2009.12.003
42. Shyh-Jier H, Cheng-Tao H, Ching-Lien H (1999) Application of Morlet wavelets to supervise power system disturbances. Power Deliv IEEE Trans 14(1):235–243. doi:10.1109/61.736728
43. Soderstrom T, Stefanovska A, Veber M, Svensson H (2003) Involvement of sympathetic nerve activity in skin blood flow oscillations in humans. Am J Physiol Heart Circ Physiol 284(5):H1638–H1646. doi:10.1152/ajpheart.00826.2000
44. Sokolnicki LA, Roberts SK, Wilkins BW, Basu A, Charkoudian N (2007) Contribution of nitric oxide to cutaneous microvascular dilation in individuals with type 2 diabetes mellitus. Am J Physiol Endocrinol Metab 292(1):E314–E318. doi:10.1152/ajpendo.00365.2006
45. Stefanovska A, Bracic M, Kvernmo HD (1999) Wavelet analysis of oscillations in the peripheral blood circulation measured by laser Doppler technique. IEEE Trans Bio-Med Eng 46(10):1230–1239
46. Tooke JE (1996) Peripheral microvascular disease in diabetes. Diabetes Res Clin Pract 30(Suppl):61–65
47. Tsukada K, Hase K, Minamitani H, Sekizuka E, Oshio C (2001) Simultaneous measurement of blood flow distribution and oxygen tension by photoexcitation in organ microcirculation. Trans Inst Electr Eng Jpn Part C 121-C(9):1415–1421
48. Veves A, Akbari CM, Primavera J, Donaghue VM, Zacharoulis D, Chrzan JS, DeGirolami U, LoGerfo FW, Freeman R (1998) Endothelial dysfunction and the expression of endothelial nitric oxide synthetase in diabetic neuropathy, vascular disease, and foot ulceration. Diabetes 47(3):457–463
49. Vinik AI, Erbas T, Park TS, Stansberry KB, Scanelli JA, Pittenger GL (2001) Dermal neurovascular dysfunction in type 2 diabetes. Diabetes Care 24(8):1468–1475
50. Ward JD, Boulton AJ, Simms JM, Sandler DA, Knight G (1983) Venous distension in the diabetic neuropathic foot (physical sign of arteriovenous shunting). J R Soc Med 76(12):1011–1014

51. Williams SB, Cusco JA, Roddy MA, Johnstone MT, Creager MA (1996) Impaired nitric oxide-mediated vasodilation in patients with non-insulin-dependent diabetes mellitus. J Am Coll Cardiol 27(3):567–574
52. Yazdanfar S, Rollins AM, Izatt JA (2000) In vivo imaging of blood flow dynamics using color Doppler optical coherence tomography. In: Coherence domain optical methods in biomedical science and clinical applications IV, 24–26 Jan 2000, USA. Proceedings of the SPIE—International Society Optics Engineering (USA). SPIE Int Soc Opt Eng, pp 106–111. doi:10.1117/12.384146
53. Zioupos P, Barbenel JC, Lowe GDO, MacRury S (1993) Foot microcirculation and blood rheology in diabetes. J Biomed Eng 15(2):155–158. doi:10.1016/0141-5425(93)90048-4